Document downloaded from:

http://hdl.handle.net/10251/104483

This paper must be cited as:

Marcos-García, P.; Lopez-Nicolas, A.; Pulido-Velazquez, M. (2017). Combined use of relative drought indices to analyze climate change impact on meteorological and hydrological droughts in a Mediterranean basin. Journal of Hydrology. 554:292-305. doi:10.1016/j.jhydrol.2017.09.028

The final publication is available at

https://doi.org/10.1016/j.jhydrol.2017.09.028

Copyright Elsevier

Additional Information

Combined use of relative drought indices to analyze climate change impact on meteorological and hydrological droughts in a Mediterranean basin

Marcos-Garcia, P[1*], Lopez-Nicolas, A.[1], and Pulido-Velazquez, M.[1]

[1]Research Institute of Water and Environmental Engineering (IIAMA), Universitat Politècnica de València, Camí de Vera s/n 46022 Valencia, Spain.

*Corresponding author: patmarg5@upv.es *(P. Marcos-Garcia), anloni@upv.es (A. Lopez-Nicolas), mapuve@hma.upv.es (M. Pulido-Velazquez)

Abstract

Standardized drought indices have been traditionally used to identify and assess droughts because of their simplicity and flexibility to compare the departure from normal conditions across regions at different timescales. Nevertheless, the statistical foundation of these indices assumes stationarity for certain aspects of the climatic variables, which could no longer be valid under climate change. This contribution provides a framework to analyze the impact of climate change on meteorological and hydrological droughts, considering shifts in precipitation and temperature, adapted to a Mediterranean basin. For this purpose, droughts are characterized through a combination of relative standardized indices: Standardized Precipitation Index (rSPI), Standardized Precipitation Evapotranspiration Index (rSPEI) and a Standardized Flow Index (rSFI). The uncertainty and the stationarity of the distribution parameters used to compute the drought indices are assessed by bootstrapping resampling techniques and overlapping coefficients. For the application of the approach to a semiarid Mediterranean basin (Jucar River Basin), the Thornthwaite scheme was modified to improve the representation of the intra-annual variation of the potential evapotranspiration and low flow simulation in hydrological modelling was improved for a better characterization of hydrological droughts. Results for the Jucar basin show a general increase in the intensity and magnitude of both meteorological and hydrological droughts under climate change scenarios, due to the combined effects of rainfall reduction and evapotranspiration increase. Although the indicators show similar values for the historical period, under climate change scenarios the rSPI could underestimate the severity of meteorological droughts by ignoring the role of temperature.

Keywords: standardized drought indices, climate change impact, meteorological droughts, hydrological droughts, evapotranspiration.

1. Introduction

Unlike aridity, a permanent feature of climate in low rainfall areas, droughts are temporary deviations that can happen in any climatic region (Wilhite 2000; Tallaksen & Van Lanen 2004). Droughts, generally defined as divergences from normal conditions on water availability, often start with a prolonged lack of precipitation and then propagate to other components of the hydrological cycle. Persistent droughts can lead to a significant depletion of reservoirs' storages and groundwater levels, with a subsequent broad range of socio-economic and environmental impacts. According to the latest report of the Intergovernmental Panel on Climate Change (IPCC, 2014a), the current emission of greenhouse gases will increase global warming and produce durable changes in the climate system, raising the likelihood of extreme events. Under those conditions, droughts could become more frequent and severe around the world (Dai, 2013), with a growing impact on water resources. In this context, the Mediterranean region emerges as a prominent regional climate change hotspot

(Diffenbaugh and Giorgi, 2012). The most relevant key climatic drivers for water availability are precipitation, temperature, evaporative demand (which depends on net radiation), atmospheric humidity, wind speed and temperature (Bates et al., 2008). The current climate models are able to reproduce the observed continental-scale surface temperature patterns and trends with assurance, but the level of performance for large scale patterns of precipitation is lower than that of temperature (IPCC, 2014b). This fact poses high uncertainty regarding future climate projections and therefore, on the effects of climate change on drought severity at the regional level (Burke and Brown, 2007). Particularly in areas with high precipitation variability, such as the Mediterranean region, the drought patterns derived from the outputs of global climatic models are not consistent (Vicente-Serrano et al., 2004).

In recent years, many studies have been conducted to assess the potential impact of climate change on meteorological, agricultural and hydrological droughts in different regions of the world, using different indicators depending on drought types (e.g. reviews by Mishra and Singh, 2010; Zargar et al., 2011; Pedro-Monzonis et al., 2015). Most of these studies are conducted using well-established indices, such as the Palmer Drought Severity Index (PDSI; Palmer 1965), based on soil water balance equation, or the Standardized Precipitation Index (SPI; McKee et al., 1993), based on a probabilistic approach for precipitation to evaluate meteorological droughts. Although the benefits and drawbacks of these indices for the analysis of historical droughts have been widely discussed (Alley, 1984; Dai, 2011; Hayes, 1999), few authors have addressed the specific limitations of the traditional indicators under a nonstationary, climate change context. Vicente-Serrano et al. (2010) pointed out the inability of SPI to identify the role of global warming in future drought conditions, since it neglects the effect that a temperature increase and subsequent evapotranspiration increase can have on droughts. To overcome this issue, they propose a new climatic drought index (the

Standardized Precipitation Evapotranspiration Index (SPEI)), which combines the sensitivity of PDSI to changes in evaporation demand (caused by temperature fluctuations and trends) with the simplicity of calculation and the multi-temporal nature of the SPI. Nevertheless, it is important to note that potential evapotranspiration (PET) formulations introduce additional uncertainty to that due to the climate models (Kay and Davies, 2008). The use of standardized drought indices is appealing for many reasons: the procedure is simple and can be generalized for assessing different types of droughts (e.g. Shukla and Woods, 2008), they are comparable in time and space (Hayes, 1999). Nevertheless, the traditional statistical foundation of these indices cannot be used in climate change impact assessments, as they would provide approximately the same distributions for both present and changed climates regardless of the changes in the climate conditions (Dubrovsky et al., 2009; Zargar et al., 2014).

In this paper we study the impacts of climate change on meteorological and hydrological droughts in a Mediterranean basin through a combination of relative standardized indices that allow for the consideration of predicted shifts in precipitation and temperature. For dealing with the uncertainty on the parameters of the distributions used to compute the drought indices, bootstrapping techniques are applied to compute the overlapping coefficient (OVL) for each parameter between the historical and future density functions. The catchment and climate characteristics of the case require modifications to the method for PET estimation and to the conceptual hydrological simulation model (improved simulation of low-flow conditions to better represent hydrological droughts). The catchment characteristics help to explain the spatial differences on the historical and future drought characteristics.

In the upcoming sections, the overall approach and its adaptation to the sui-generis characteristics of a Mediterranean basin are presented. Then, drought characterization under climate change conditions using standardized relative indices is explained. The study area, the climate change projections, and the bias correction method are described. The specific modifications for adapting the method to the case study, including the hydrological simulation and the PET estimation methodology are presented. Finally, the paper shows the main results, the discussion and the main conclusions are presented.

2. Method

2.1. Overall approach

The selected methodology (Fig. 1) involves three main steps: future time series generation, hydrological modeling and drought assessment.

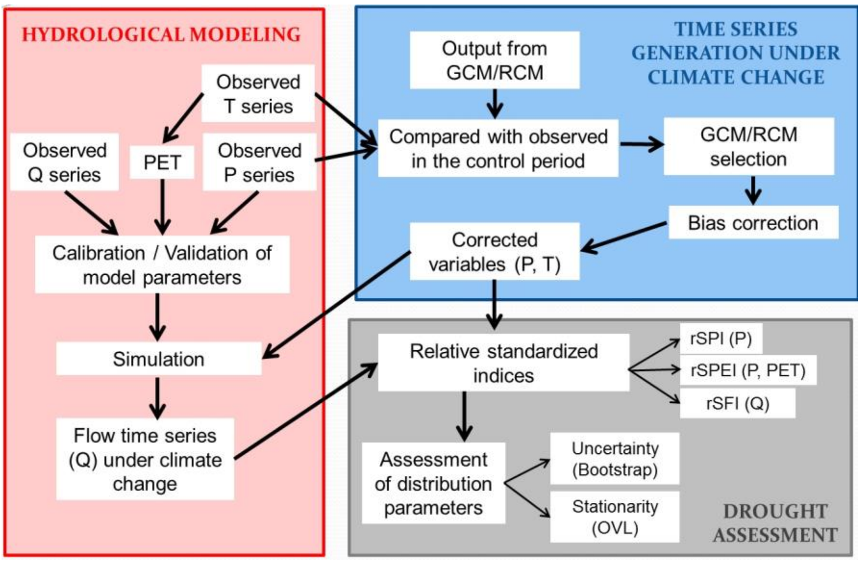

Fig. 1. Overall approach scheme

A) <u>Time series generation under climate change</u>:

This step first requires selecting a set of climate change projections, using the outputs from a combination of Global Circulation Models (GCMs) and Regional Circulation Models (RCMs). These future projections are based on the new IPCC scenarios, the Representative Concentration Pathways (RCPs), which define four different pathways of greenhouse emissions and atmospheric concentrations, air pollutant emissions and land use (IPCC, 2014b). The main advantage of the new RCP scenarios over the Special Report Emissions

(SRES) scenarios is that the impacts of the international agreements and efforts to mitigate the gas emissions are considered.

GCMs reproduce physical processes and the effect of an increase of greenhouse gases concentration in the climate system. Nevertheless, GCMs present the disadvantage of scale or resolution, normally having a horizontal resolution of between 250 and 600 km, 10 to 20 vertical layers in the atmosphere (IPCC, 2014a). For this reason, the Regional Climate Models (RCMs) are used to perform the climate change projections with more accuracy at the local level, through downscaling techniques. The selection is made based on the goodness-of-fit between the observed and the simulated values for the control period.

Although RCMs downscale the outputs of GCMs, precipitation and temperature simulations from RCMs are known to be biased and need to be post-processed in order to produce reliable estimates of expected local climate conditions (Fowler et al., 2007). Several bias correction methods have been developed, mostly based on statistical transformations to adjust selected aspects of the distribution of RCMs so that the new distribution resemble the original (e.g., Teutschbein and Seibert 2012; Gudmunsson et al. 2012). In this research we apply the equidistant "quantile mapping" method (Li et al., 2010) to correct the bias of future climatic projections by adjusting the cumulative distribution function (CDF) for the future period based on the difference between the model and the observed CDFs for the control (baseline) period. The method has been proved to be more efficient in reducing biases than the traditional CDF mapping method for changing climates, especially for the tails of the distribution (Li et al., 2010). For the implementation of the bias correction process, we used the statistical package "qmap" for post-processing the climate model output (Gudmunsson et al., 2012). The tool, implemented in R statistical software (R development team, 2015), allows to use different fitting options and to select the transformation for modelling the quantile-quantile relation between the observed and the modelled time series, choosing quantiles that are regularly spaced through least-square regression.

B) Hydrological modeling:

To assess the climate change impacts on hydrological droughts, it is necessary to simulate future flows (river discharges), using the bias corrected temperature and precipitation variables as inputs to a hydrological model. The most simple and straightforward method to estimate the potential evapotranspiration (PET) is the Thornthwaite model. However, as discussed in Section 4.3, this approach has some drawbacks when applied to semiarid areas, where it may underestimate the PET. In our case, we apply a conceptual, lumped-parameter Temez model, modified to improve the representation of low flows, which is essential in the characterization of hydrological droughts. The application of this methodology to the case study is further developed in Sections 4.2 and 4.3.

C) Drought assessment:

Drought analysis is based on the use of relative standardized indices (rSPI, rSPEI and rSFI) and the "run theory" (Yevjevich, 1967; Dracup et al., 1980) to obtain main drought properties (magnitude, duration and intensity). One possible approach to tackle nonstationarity of hydrologic extremes is to assume that, at any given time, an extreme value distribution would still be used, but the distribution itself would shift over time (Coles 2001; Katz 2013; Salas and Obeysekera 2014). For this reason, these authors introduced nonstationarity by expressing one or more of the parameters of the GEV distribution as a function of time. The uncertainty of SPI's model parameters was addressed by Zargar et al. (2014), who proposed the generalization of the traditional deterministic definition to an uncertainty-driven one, capable of modeling both sources of uncertainty: aleatory (effect of climate change on variability) and epistemic (limited knowledge about the system). Here we propose a methodology to characterize both the uncertainty of the SPEI assumed distribution parameters and the level of agreement between the historical and the future density function of these parameters, in order to assess shifts in the distribution under climate change scenarios. In this regard, we suggest that, whenever a low level of agreement exists, the parameter could be considered as nonstationary.

2.2. Standardized drought indices

In the present paper, drought definition is based on three standardized indices: the Standardized Precipitation Index (SPI), the Standardized Precipitation and Evapotranspiration Index (SPEI) to assess meteorological droughts, and the Standardized Runoff or Flow Index (SFI), which are applied to river discharge to analyze hydrological droughts. Although the original standardization procedure was defined for the SPI (McKee et al., 1993) using the precipitation as variable, the calculation of the SPEI and SFI indices follows the same process but changing the variable to standardize: the difference between precipitation and PET (climatic water balance) for the SPEI, and streamflow for the SFI. The steps involved in the procedure are:

1. Time window selection: this window will reflect specific impacts and phenomena of interest. According to Zargar et al. (2011), specific aggregation periods for the SPI could be used to characterize different phenomena. Shorter SPI aggregation periods (3-6 months) could be used to obtain seasonal estimations of precipitation, as they represent short and medium-term moisture conditions and medium-term trends in precipitation, respectively. However, 12 month SPI is able to reflect long-term precipitation patterns, and it could be tied to streamflows, reservoir levels and also groundwater levels. The time window selection is further developed in Section 4.4.

2. Fitting of a statistical distribution to the time series: McKee et al. (1993) originally fitted the gamma distribution to the precipitation data series to compute the SPI. This 2-parameter distribution can also be applied to the streamflow series to obtain the

SFI, although it is not necessarily the best choice (Barker et al., 2015). Moreover, the gamma distribution cannot be used for the SPEI, because the climatic water balance is not bounded by zero and may take negative values if PET exceeds precipitation. Therefore, a 3-parameter distribution is required to compute the SPEI. Vicente-Serrano et al. (2010) originally proposed the log-logistic distribution for the SPEI computation, but recently Stagge et al. (2015) suggested that the generalized extreme value (GEV) distribution produced the best goodness-of-fit across different accumulation periods for the SPEI. Mathematically, the GEV distribution is very attractive because its inverse has a closed form and the parameters are easily estimated by moments (Hosking et al., 1985). In this case, we apply the well-tested gamma distribution to the precipitation and streamflow series to obtain the SPI and the SFI, respectively, and the GEV distribution to compute the SPEI.

3. Transformation to a standardized normal distribution: using an equi-percentile transformation, the selected cumulative probability function has to be transformed into a standard normal random variable with mean 0 and standard deviation 1. Therefore, the standardized indices are representations of the number of standard deviations of departure from the mean at which an event occurs (often called “score”).

Using these scores, drought intensity can be further categorized. Instead of the original categories defined by McKee et al. (1993) for the SPI, we have adopted the classification suggested for the same index by Agnew (2000) (Table 1). This approach gives a lower probability of occurrence to the more severe droughts, unlike the original thresholds proposed by McKee (1993), which assigned some type of drought to all the negative SPI indices.

Table 1. Drought categories through SPI values (adapted from Agnew, 2000)

SPI values			Drought Categories
0	to	-0.84	No drought
-0.84	to	-1.28	Moderate
-1.28	to	-1.65	Severe
	<	-1.65	Extreme

Finally, we apply the run theory (Yevjevich, 1967) to obtain two additional drought properties: duration and magnitude. A drought is considered as a run of deficits (time series values below a threshold). For each drought episode, duration is defined as run length, magnitude as run sum (cumulative deficit) and intensity as the maximum deficit in a run (Dracup et al., 1980).

2.3. Drought characterization under climate change

2.3.1 Relative indices

Dubrovsky et al. (2009) found that the SPI provided approximately the same distributions for both present and changed climates regardless of the changes in the climate conditions. To solve the problem, they proposed the use of a “relative SPI” (rSPI) instead of the traditional SPI. Traditional indices computation involves the estimation of different distribution parameters for the historical data and for each of the future time series. Fig. 2 represents the SPI values computed in Sueca sub-basin for the historical time series (520 mm per year on average) and for the RCP 8.5 midterm scenario (402 mm per year), considering a temporal aggregation of 12 months. We can observe that the range of SPI values is about the same for the historical data and for the future time series, despite a rainfall reduction of 22.7%.

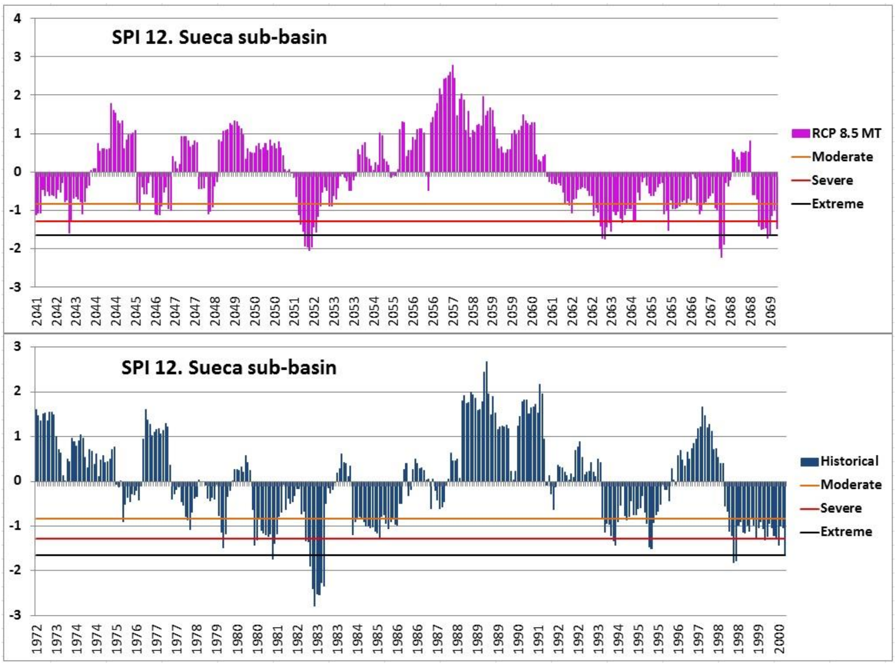

Fig. 2. SPI 12 for historical data (years) and RCP 8.5 midterm scenario (MT). Sueca sub-basin.

In contrast, for the relative SPI (Dubrovsky et al., 2009), the parameters k and θ of the gamma distribution are obtained for a certain reference weather series (historical data) and then the same distribution is applied to tested series (future conditions). Fig. 3 shows the relative SPI in Sueca sub-basin for the RCP 8.5 midterm scenario and a temporal aggregation of 12 months. Unlike Fig. 2 (traditional SPI), the rSPI identifies multiple and long-lasting extreme drought spells for these future conditions, although the temporal structure is the same for both indices.

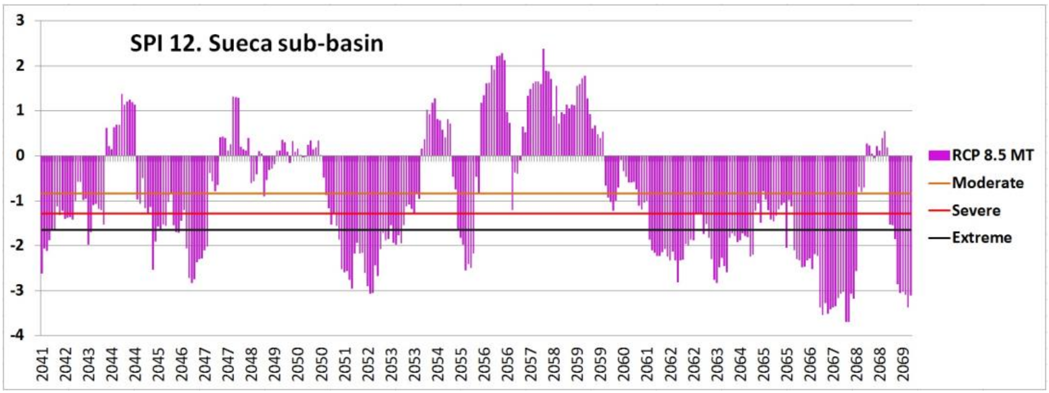

Fig. 3. Relative SPI 12 for RCP 8.5 midterm scenario. Sueca sub-basin.

Here, we apply the same approach to compute relative SPI (rSPI), relative SPEI (rSPEI) and relative SFI (rSFI) in the basin. The use of the rSPEI in addition to the rSPI for meteorological droughts allows to assess the effect that the increase in temperature and subsequently in ET can have on drought severity (Vicente-Serrano et al., 2010; Beguería et al., 2014). In the case of the rSPEI, it is important to note that the 3-parameters distribution functions considered for the SPEI calculation have a location parameter. This fact means that the distribution fitted to the reference series may not be defined for certain values of the tested series, as it happens for the 3-parameter log-logistic distribution when the value of the variable is less than the location parameter of the distribution. Nonetheless, this limitation can be addressed through the selection of proper limits for the index, considering that if the distribution is not defined for the value or it is under/above the limit, this merely indicates that the effective precipitation is very small/large.

2.3.2 Assessment of uncertainty and nonstationarity in the probability distributions of the SPEI parameters

For the uncertainty-driven SPEI, epistemic uncertainty in parameter estimation has been assessed using the bootstrap resampling method (Efron, 1979). Concretely, a parametric bootstrap has been performed using the package "boot" of the R statistical software (Canty et al., 2015) to compute the sampling density function of each parameter. The magnitude of variability with regard to epistemic uncertainty is introduced through the overlapping coefficient (OVL), which measures the agreement between the density function of the parameter for the historical period and the density function of the same parameter for future scenarios. The reason for selecting the OVL for the comparison of density functions is that it is easy to interpret. Of the three possible OVL described in literature (Matusita's measure ρ, Morisita's measure λ and Weitzman's measure Δ), we have selected the last one (Weitzman, 1970), which is the most commonly used (Eq. 1):

$$\Delta = \int \min\left\{ f_1(x), f_2(x) \right\} dx \qquad [1]$$

Where f1(x) and f2(x) are two probability density functions.

3. Material

3.1. Case study

The case study is the Jucar River Basin, a Mediterranean basin of 22261 km^2 in Eastern pain (Fig. 4). The system is highly regulated, with a share of water for crop irrigation about 80%. The main consumptive water demands, concentrated in the lower basin (except for groundwater irrigation in Mancha Oriental, in the upper basin), are of irrigation and urban water supply. Water scarcity, irregular hydrology and groundwater overdraft cause droughts to have significant economic, social and environmental consequences. Most surface water resources are regulated through the 3 main surface reservoirs: Alarcon and Contreras, in parallel in the upper basin, and Tous, downstream. There is a vulnerable equilibrium between available resources (1798 million of m^3 is the average annual inflow from 1940/41 to 2011/12) and total demand (1640 million of m^3) (CHJ, 2015). The Jucar river basin has been split into 9 sub-basins (Fig. 1) in order to characterize the spatial variability of droughts in the system. The division was done according to the drainage network of the system, location of main reservoirs, climatic characteristics, and data availability.

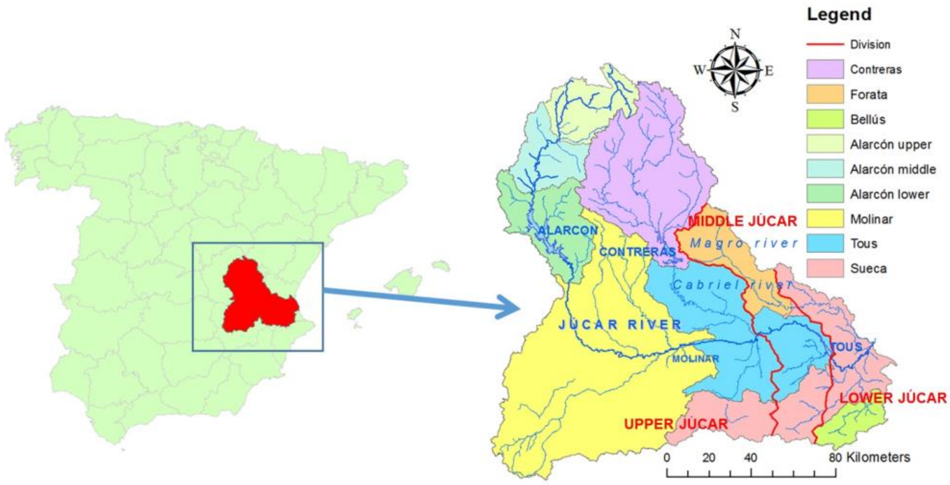

Fig. 4. Location of the Jucar river basin (left) and sub-basins (right)

Three geographical areas can be identified in the basin regarding climatology. The upper Jucar presents a continental climate, with mean precipitation of 630 mm/year and mean air temperature of 11.6^{o}C. The area includes the catchment draining to the Alarcon reservoir in the Jucar river (mean annual flow of 396.1 million of m^3/year, 1940/41-2011/12), the catchment of the Cabriel river, its main tributary (mean annual flow of 342.1 million of m^3/year, 1940/41-2011/12), and the catchment of the Mancha Oriental aquifer, an extensive carbonate aquifer (7260 km^2) hydraulically connected to the river. Intense overpumping in the last decades for irrigation has led to a significant drop in the water table, with the consequent streamflow depletion in the Jucar river (Sanz et al., 2011). Understanding the behavior of this stream-aquifer interaction is essential for characterizing the hydrology of the basin, and particularly, the low flow situations.

The Mid Jucar region presents a mild climate (between the continental and Mediterranean climates), extending from Embarcaderos to the Tous dam in the Jucar river and including the Magro, Albaida and Sellent basins. Finally, the Lower Jucar, downstream the Tous dam, presents a typical Mediterranean coastal climate, with mean precipitation of 450 mm/year and mean air temperature of 17^{o}C (CHJ, 2015). The river basin has suffered several significant droughts in the last 60 years, registering the most severe dry spells in the last two decades:

from 1991/92 to 1994/95 (average SPI of -1.02), from 1997/98 to 1999/00 (average SPI of -1.13) and from 2004/05 to 2007/08 (average SPI of -1.08) (CHJ, 2007). Several previous studies have evaluated the impact of climate and land use changes in the Jucar basin or sub-basins (e.g. Pulido-Velazquez et al., 2015; Pérez-Martín et al., 2015; Marcos-Garcia and Pulido-Velazquez, 2017;).

3.2 Historical and climate change data

In order to characterize climatic variables for the historical control period (1971-2000), daily precipitation and temperature were obtained from the SPAIN 02 project (Herrera et al., 2010), with high-spatial resolution (0.11^{o}). Monthly discharge time series data at the gauging stations at the outlet of each sub-basin, previously transformed into impaired flow, were used for the calibration and validation of the hydrological model.

We used the outputs from the CORDEX project to get the future time series of precipitation and temperature, through the Earth System Grid Federation platform (ESGF). CORDEX evaluates and improves regional climate downscaling models and techniques, producing a great range of sets of regional downscaled projections all over the world (Christensen et al., 2014).

The gross climatic projections have been obtained for three periods of time: control period (1971-2000), short-term period (2011-2040) and mid-term period (2041-2070). In this study we selected RCP 4.5 and RCP 8.5 scenarios in order to include a medium and a high, more extreme emission scenario.

4. Application

4.1. Climate change scenarios

Results from different combinations of GCMs and RCMs (Table 1 at supplementary material, spatial resolution of 0.44^{o}) have been analyzed in order to select the most suitable climate model. The monthly average precipitation and temperature time series for the control period (1970-2000) have been compared (Fig. 5), obtaining that the simulated precipitation from the combination of the GCM simulations from the Canadian Centre for Climate Modelling and Analysis (CCCmaCanESM2) and RCA4 (as RCM) provides the best fit to the observed monthly precipitation during the control period. This GCM-RCM combination also shows a good performance in reproducing the observed average monthly temperature for the control period. For those reasons, it has been the selected combination in the present study.

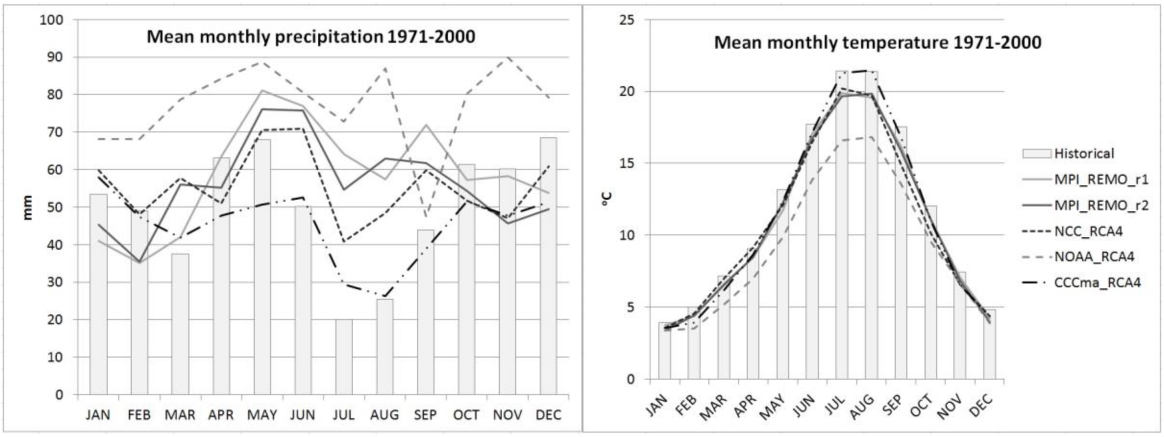

Fig. 5. Observed vs simulated (climate models) monthly average rainfall and temperature of the control period

4.2 Hydrological modelling with improved low flow simulation

The hydrological simulation has been implemented through a set of monthly Temez models (Temez, 1977) for the 9 sub-basins in which the study area is divided into (Fig. 4). The Temez hydrological model (Temez, 1977) is a conceptual, deterministic and continuous monthly water balance model, lumped and with few parameters (just 4), which has been widely used for water resources assessment in Spain (Estrela et al., 1999).

In this study we have modified the original formulation of the Temez model to improve the representation of the low-flow conditions (the hydrograph recessions), what is essential in the characterization of hydrological droughts (Fig. 6). The recession limb in a hydrograph easily deviates from a single exponential law or single linear reservoir model (Tallaksen, 1995).

Mathematically, the structure of the stream-aquifer interaction can be conceptualized as the drainage of an infinite number of independent linear reservoirs (Pulido-Velazquez et al., 2005). In most practical problems, stream-aquifer flow exchange can be accurately reproduced with few linear reservoirs (Pulido-Velazquez et al., 2005), even in the case of complex karstic aquifers (Estrela and Sahuquillo, 1985). In this case, we use 2 linear reservoirs to improve the representation of the low-flow, recession conditions. The aquifer is modeled as two independent linear reservoirs, in which groundwater discharge from each reservoir or tank is linearly proportional to the storage V(t) above its outlet, with α_i (groundwater discharge or recession coefficient) as the proportionality factor. The recharge is shared between the two tanks according to a certain allocation factor to be calibrated. The variation introduces two additional parameters (a second recession coefficient and an allocation factor to distribute the recharge between the two tanks) and one additional state variable (volume stored in the second tank).

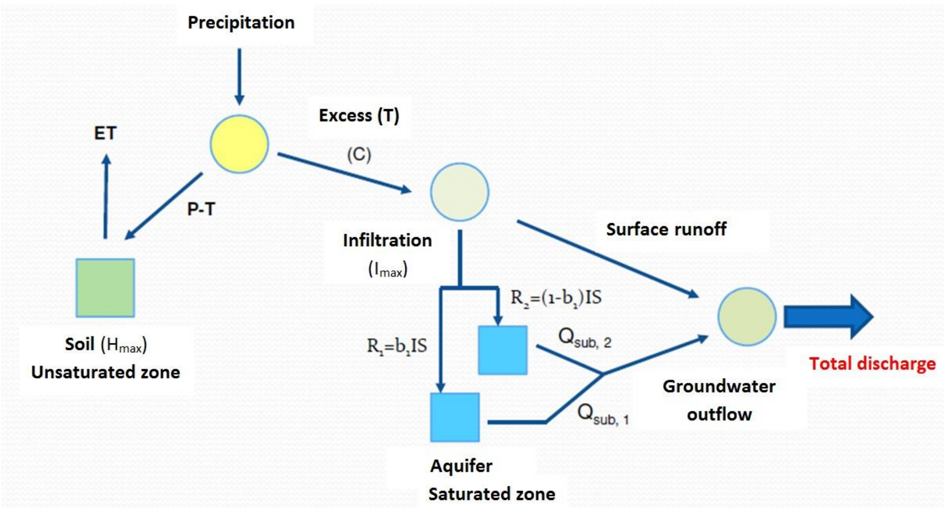

Fig. 6. Temez model scheme considering the aquifer as two linear reservoirs.

The model has been calibrated for the 9 sub-basins using monthly discharge data from the gauging stations at the outlet of each sub-basin for the period 1971-2000, previously transformed into natural flow using historical data of water use in the basin (provided by the river basin authority) and nonlinear optimization to minimize an indicator of the goodness-of-fit between the observed and the simulated time series. The validation has been carried out for the period 2001-2007. Table 2 shows the goodness of fit of the hydrological model for the different sub-basins, using the original formulation (sub-index 1) and the modified procedure (sub-index 2). We can observe that the overall performance of the modified procedure overtakes the one of the original formulation.

Table 2. Goodness of fit of the hydrological models

Calib.	**Alarcón upper**	**Alarcón middle**	**Alarcón lower**	**Contreras**	**Molinar**	**Tous**	**Sueca**	**Forata**	**Bellús**
NSE_1	0.78	0.81	0.73	0.65	0.50	0.58	0.54	0.67	0.77
NSE_2	0.84	0.82	0.73	0.73	0.50	0.60	0.61	0.75	0.75
R_1	0.89	0.90	0.91	0.81	0.71	0.58	0.78	0.82	0.88
R_2	0.91	0.90	0.91	0.86	0.71	0.60	0.80	0.87	0.89
$LNSE_1$	0.61	0.82	0.89	0.64	0.42	0.58	0.56	0.25	0.79
$LNSE_2$	0.75	0.82	0.90	0.77	0.42	0.58	0.57	0.69	0.69
Valid.									
NSE_2	0.87	0.94	0.89	0.63	0.09	0.21	0.47	0.56	0.52
R_2	0.94	0.98	0.96	0.91	0.25	0.78	0.76	0.64	0.87
$LNSE_2$	0.79	0.84	0.80	0.75	0.01	0.20	0.30	0.39	0.56

The Temez model is able to properly represent the hydrology of the system, with the exception of Molinar and Tous sub-basins, with low values of the Nash-Sutcliffe coefficient. These values are not only attributable to the model's behavior, but also to the uncertainty associated with the transformation of the data registered at the gauging stations into naturalized flow. In the first case, Molinar sub-basin presents a complex interaction with the Mancha Oriental aquifer, which has changed over time due to intensive pumping. In the second case (Tous sub-basin), the two existing gauging stations have incomplete time series, with only a few common years. The model also presents a low performance during the validation period for these sub-basins. Fowler et al. (2016) argue that Split Sample Test evaluations sometimes undervalue the predictive capacity of conceptual lumped models.

4.3 Corrected potential evapotranspiration

We need a simple and efficient procedure that can be applied when temperature is properly characterized throughout the river basin but there is a poor spatial definition of other climate variables. For our study area we have used gridded daily temperature datasets from SPAIN 02 project (Herrera et al., 2010) for the period 1971-2007 with high-spatial resolution (0.11°) and daily records of temperature, radiation, humidity and wind speed for the period 1999-2014 in 23 stations.

It is broadly documented that Thornthwaite's method (Thornthwaite, 1948) undervalues the potential evapotranspiration (PET) in areas of continental climate (e.g. Sellers, 1963; Trajkovic, 2005). For example, it considers that PET is null when the temperature is near zero. For that purpose, we decided to use an "effective temperature" (Tef) instead of the original average temperature (as suggested by Camargo et al., 1999), as in Eq. 2, and a correction based in the daily photoperiod (Pereira et al., 2004) (Eq. 3):

$$T_{ef} = k(T_{avg} + A) = \frac{1}{2}k(3T_{\max} - T_{\min}) \qquad [2]$$

$$T_{ef}^{*} = T_{ef}\,\frac{N}{24 - N} \qquad \text{If} \qquad T_{avg} \le T_{ef}^{*} \le T_{\max} \qquad [3]$$

Where Tef is the effective temperature, Tavg is the average daily temperature, Tmax is the maximum daily temperature, Tmin is the minimum daily temperature, A is the daily amplitude (Tmax-Tmin), k is a constant value empirically estimated and N is the photoperiod. The parameter k was calibrated by fitting the output values of the modified Thornthwaite scheme to the ones computed by Penman-Monteith equation for each of the 23 complete stations available. Nevertheless, it continues to underestimate the evapotranspiration in the continental climate zone during winter months (Fig. 7).

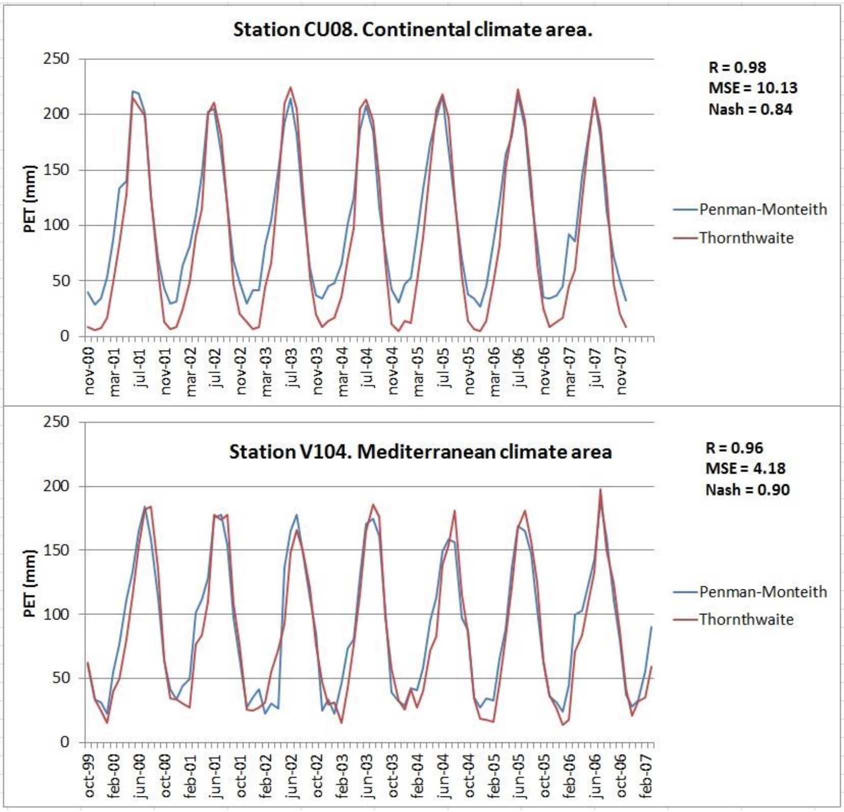

Fig. 7. Estimated PET (mm) using Penman-Monteith equation and modified Thornthwaite at two stations within different climate areas (using Eq. 2)

To overcome this issue, we propose a modification of Eq. 2 for the calculation of the effective temperature by adding a new parameter b to provide more flexibility to the scheme (Eq. 4)

$$T_{ef} = a(T_{avg} + A)^{1-b} \qquad [4]$$

Where Tavg is the average daily temperature, A is the daily amplitude and a and b are parameters. For the case study, we have generally obtained a good fit using values of a=4.5 and b=0.5. The suggested formula was able to properly represent the intra-annual variation of PET within the continental climate area, even during the coldest months (Fig. 8). With regards to the stations located in the Mediterranean climate, there is little improvement under the new version (Fig. 8).

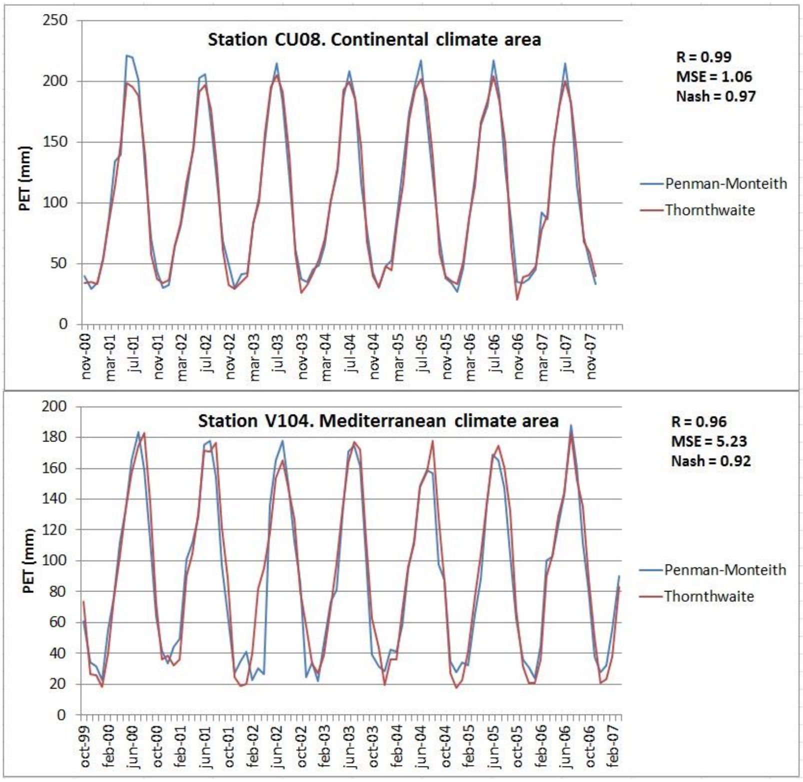

Fig. 8. Estimated PET (mm) using Penman-Monteith equation and modified Thornthwaite scheme at two stations within different climate areas (using Eq. 4)

4.4. Time window selection

We used the Anderson test to find that the annual autocorrelation is statistically significant (Fig. 1 at Supplementary material). We also analyzed the autocorrelation for time lags of 3 (0.18), 6 (0.12) and 12 months (0.21). Since the highest autocorrelation is for an aggregation period of 12 months, this was the temporal lag selected.

5 Results

5.1 Historical droughts

The results for both the SPI and SPEI indices are very similar within the historical period (1971-2000). As an example, Fig. 9 shows SPI vs SPEI for Contreras sub-basin (upper Jucar).

Therefore, SPI could be a suitable drought indicator during this period in the Jucar river basin, even though it ignores the role of temperature.

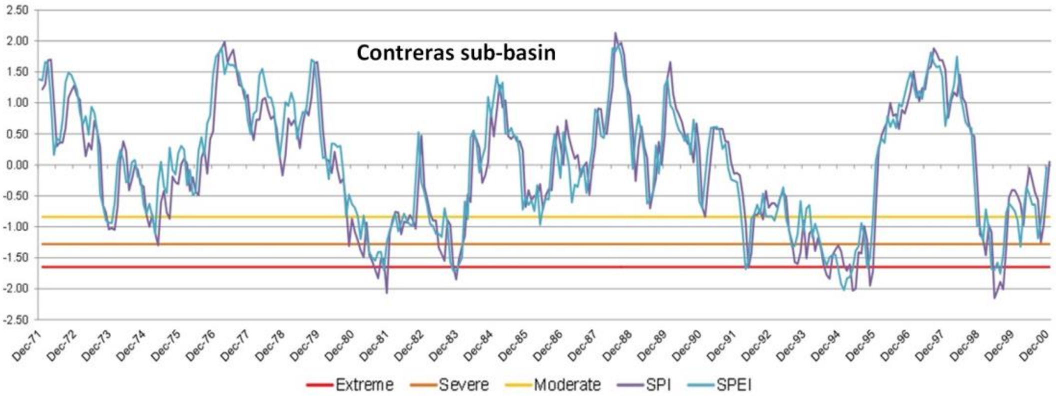

Fig. 9. Historical SPI12 and SPEI12 in the Contreras sub-basin (upper Jucar)

The run theory has been applied to the SPI historical time series for assessing the magnitude, intensity and duration of droughts (Table 3). The table reveals that in general, the mid (Tous) and lower (Forata, Bellus and Sueca) basins present longer and more severe (in magnitude and intensity) droughts than the upper Jucar (Alarcon and Contreras). This is consistent with the distribution of the main climatic areas in the basin (continental climate in the upper Jucar, transitional continental-Mediterranean in the mid basin, and typical Mediterranean in the lower basin).

Table 3. Analysis of historical meteorological droughts based on the SPI12

	Number of droughts	Average magnitude	Average Duration	Average Intensity	Drought category
Contreras	10	14.92	16.10	1.32	Severe
Alarcon upper	12	11.36	14.25	1.23	Moderate
Alarcon middle	14	9.51	11.36	1.21	Moderate
Alarcon lower	9	16.52	16.67	1.45	Severe
Molinar	10	12.37	13.90	1.40	Severe
Tous	2	25.95	26.50	1.70	Extreme
Bellus	8	19.99	20.38	1.46	Severe
Forata	10	15.00	17.50	1.37	Severe
Sueca	8	16.01	17.25	1.46	Severe

The magnitude, intensity and duration of hydrological droughts derived from the Standardized Flow Index (SFI), unlike the meteorological droughts, cannot be directly linked to the main climatic areas in the Jucar river basin. Maximum mean drought magnitude, intensity and duration values could be observed in both, the upper (Contreras) and lower basin (Bellus, Sueca) (Table 4). As expected, the number of hydrological droughts is lower than the number of meteorological droughts, since not all meteorological droughts end up generating hydrological droughts. But, once a hydrological drought happens, its duration and magnitude overcome those of the meteorological drought. For example, in Contreras sub-basin, 10 meteorological droughts are identified against only 4 hydrological droughts. However, the average magnitude of the meteorological droughts is 14.92, while for hydrological droughts is more than twice (37.49).

Table 4. Analysis of historical hydrological droughts based on the SFI12

	Number of droughts	Average magnitude	Average Duration	Average Intensity	Drought category
Contreras	4	37.49	39.25	1.45	Severe
Alarcon upper	8	16.72	20.50	1.18	Moderate
Alarcon middle	6	18.71	25.50	0.91	Moderate
Alarcon lower	6	18.63	25.83	1.00	Moderate
Molinar	4	20.85	45.75	0.72	No drought
Tous	3	15.49	18.00	1.43	Severe
Bellus	5	32.06	36.40	1.52	Severe
Forata	8	17.25	22.50	1.19	Moderate
Sueca	4	35.00	44.75	1.40	Severe

5.2 Droughts under climate change scenarios

5.2.1 Drought analysis using relative indices

Meteorological droughts were identified using the relative SPI (rSPI). In all cases, the worst scenario is the RCP 8.5 mid-term, which produces a higher increase in magnitude, more than 50 % greater than for the historical period (Fig. 10). It is important to note that, although the number of dry spells decrease in future scenarios, the average duration and intensity increases. Particularly, in Molinar sub-basin, the rSPI identifies a single dry spell that covers the entire analysis period for each scenario with the highest magnitude by far regarding the rest of sub-basins.

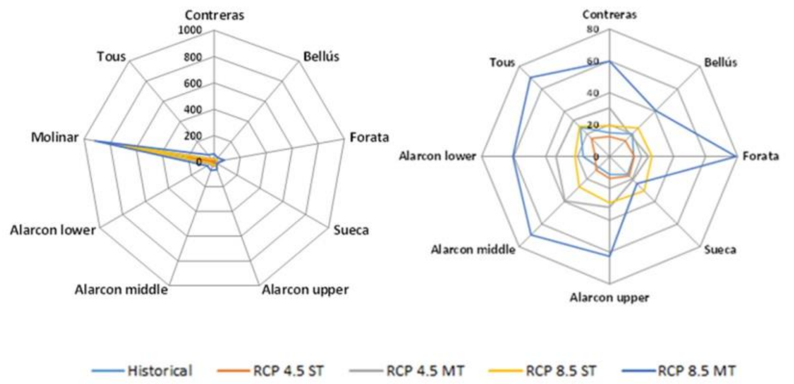

*The figure on the right excludes Molinar sub-basin to highlight the values of the rest of sub-basins

Fig. 10. Meteorological droughts, average magnitude (rSPI12) in the short term (ST) and in the midterm (MT).

To evaluate the role of the temperature increase in future droughts, the relative SPEI (rSPEI) was also computed and compared with rSPI for each sub-basin. Fig. 11 shows that the rSPEI identifies more intense droughts than the rSPI: for the RCP 8.5 mid-term in Contreras sub-basin, the rSPEI average drought magnitude triples the estimated using the rSPI. This result makes clear that the effects of the future temperature increase on droughts in the basin could not be ignored, which requires moving from the classic SPI indices to the relative SPEI. The temperature rise in the scenarios would increase potential evapotranspiration, consequently enlarging the difference between SPI (which only depends on precipitation) and SPEI (which depends on precipitation minus potential evapotranspiration). Fig. 2 at supplementary material shows the drought magnitudes for the different sub-basins according to the rSPEI. In comparison with Fig. 10, it reveals that not only Molinar sub-basin presents a continuous dry spell, but also the adjacent sub-basins of Alarcon lower and Tous show the same pattern.

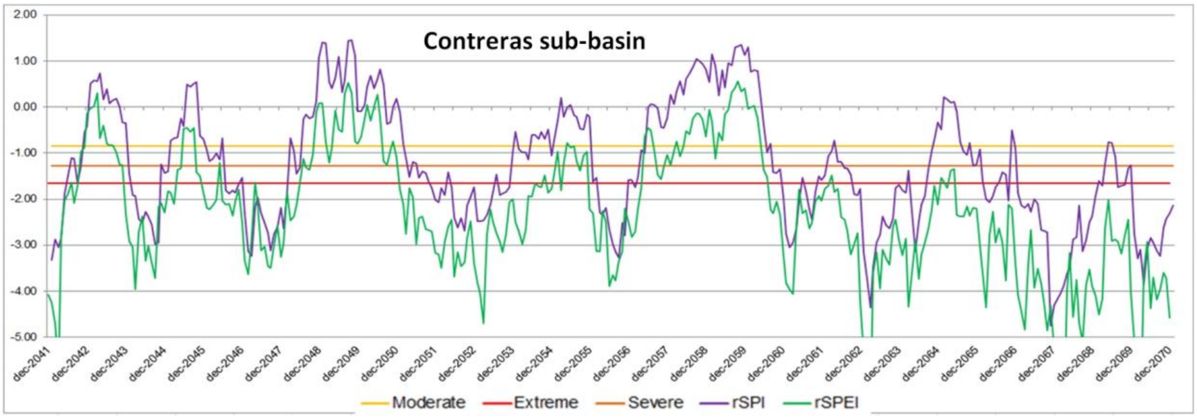

Fig. 11. Comparison between rSPI12 and rSPEI12 for Contreras. RCP 8.5 midterm

Future streamflow time series were simulated using the times series of predicted precipitation and PET (estimated from temperature as described in Section 4.3) as inputs for the Temez hydrological model at each sub-basin for the RCP 4.5 and 8.5 scenarios. Results (Fig. 12) suggest that there is a huge uncertainty regarding the future availability of water resources, although mid-term scenarios agree in a large reduction of the average annual discharge (ranging between 8-43% for RCP 4.5 and 28-45% for RCP 8.5).

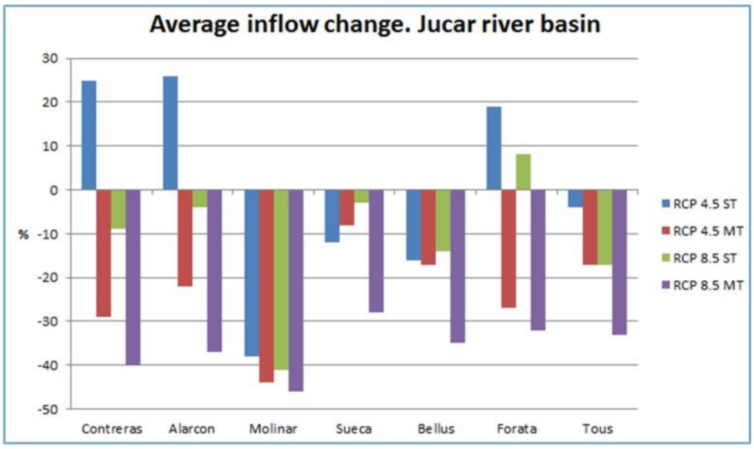

Fig. 12. Changes in average annual discharge in the short-term (ST) and in the mid-term (MT)

Hydrological drought assessment was performed calculating the relative SFI (rSFI) and then applying the run theory (Fig. 3 at supplementary material). Mid-term scenarios predict severe droughts in Contreras and Alarcon sub-basins, where the main reservoirs are located, and extreme droughts in Molinar (one of the principal recharge areas of Mancha Oriental aquifer) and Tous. For the RCP 8.5 mid-term (worst scenario), the Jucar basin would suffer a generalized extreme drought. Moreover, Molinar and Tous sub-basins would register the major hydrological drought magnitudes (cumulative deficit) increase for each scenario, as it happened when considering meteorological droughts (Fig.10).

5.2.2 Assessment of SPEI distribution parameters uncertainty and stationarity

Fig. 13 shows a comparison between the percentage of change in mean (ΔM) of the effective precipitation (P-PET) for the future scenarios with respect to the historical period, and the OVL computed for the GEV distribution parameters.

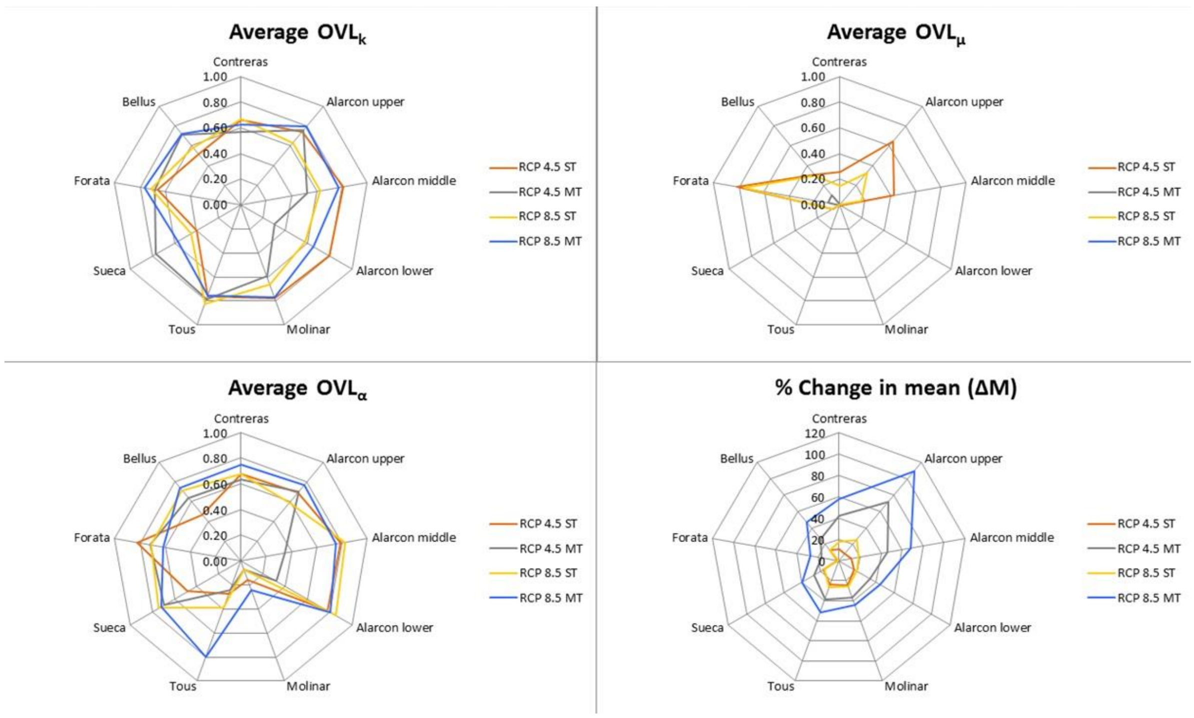

Fig. 13. Comparison between the average OVL of the distribution parameters (SPEI12) in the short-term (ST) and in the mid-term (MT)

The percentage of change in mean (ΔM) for the short-term scenarios varies between 24.27% (Molinar) and 1.11% (Forata) for the RCP 4.5, and among 26.63% (Tous) and 0.72% (Forata) for the RCP 8.5. In the mid-term, the highest ΔM occurs in Alarcon upper (more than 100%

for the RCP 8.5), and the lowest is again located in Forata sub-basin (27.25% for the RCP 8.5). For the mid-term scenarios, the OVL of the location parameter (OVLμ) is null or close to 0. Even for the short-term scenarios, OVLμ remains near 0 for the same sub-basins (lower Alarcon, Molinar, Tous and Sueca). Thus, there is no agreement between the density function of the location parameter for the historical period and the density function of the same parameter for the future scenarios. Only the upper sub-basins (Contreras, upper and middle Alarcon) and the small sub-basins of Forata and Bellus present higher values of the OVLμ for the short-term scenarios. Therefore, nonstationarity of the location parameter needs to be considered even for the short-term scenarios, with the possible exception of Forata sub-basin, which presents OVLμ values of 0.82 and 0.76 for the RCP 4.5 and RCP 8.5 short-term scenarios, respectively. Some sub-basins show high OVLα for the different scenarios (Contreras, Forata) whilst others present a low level of agreement (Molinar, Tous). Thus, the scale parameter does not shift homogeneously under climate change scenarios throughout the river basin; the convenience of considering it as time-dependent should be evaluated for each sub-basin. The shape parameter κ is difficult to estimate reliably and, for this reason, it is normally modeled as a constant (Coles 2001; Katz 2013, Salas and Obeysekera 2014). However, our results suggest that this assumption could not be appropriated in some sub-basins (Alarcon lower, Sueca), which present OVLκ values lesser than 0.5 for different scenarios. Fig. 4 at supplementary material shows the spatial distribution of the OVL values in the different scenarios.

6 Discussion

The statistical foundation of the standardized indices assumes that, for any location, certain characteristics of statistical distribution of precipitation such as the mean and distribution parameters remain stationary over time. This assumption constitutes the main limitation for the direct application of those indices to drought assessment under climate change, as they provide the same values for both present and changed climates regardless of the changes in the climate conditions. Therefore, relative standardized indices have to be used to accommodate climate change.

Two additional issues arise in the application and interpretation of the relative standardized indices. First, the selection of a proper threshold, as values outside the limits stated in current literature are frequently observed. No agreement about the thresholds for the standardized indices limits has been reached yet. McKee et al. (1993) proposed -2 and 2 as the lower and upper bounds for the SPI. Dubrovsky et al. (2009) subjectively selected these bounds to be -5.55 and 5.55, while Stagge et al. (2015) discussed the necessity of placing reasonable limits on SPI/SPEI, bounding them between -3 and 3. For our purposes, the values outside the previous stated limits were kept, since we were mainly interested in reflecting the appearance of extreme events although the values reflecting the relative severity of those events could not be accurately quantified. The second issue is the appearance of extreme dry spells over many consecutive months, which provide no information on the evolution of the dry/wet conditions. For some scenarios extreme drought seems to become a common situation whilst it should be, by definition, a temporary deviation of the normal conditions. However, it only indicates that the future variable values belong to the tails of the historical distribution and, according to this past information, have a low or even null associated probability. Future water resource systems will have to adapt to different climate conditions than those we currently know and, therefore, what we consider “normal” today may be a wet spell in the future.

When considering climate change scenarios, another uncertainty source emerges: the effect of climate change on variability, which can shift the distribution parameters over time. According to Salas and Obeysekera (2014), the scale parameter may have to be assumed as time-dependent if the upper bound of annual maxima may increase with time. Here we propose to characterize both the uncertainty of the assumed GEV distribution parameters for the SPEI and the level of agreement between the historical and the future density function of these parameters. For this reason we suggest that, if a low level of agreement exists, the parameter should be considered as nonstationary.

Results show that the overlapping coefficients for the three parameters of the GEV distribution present a wide variation throughout the river basin, and it is not possible to identify a common pattern. Nevertheless, it is important to note that OVL for the location parameter is null or close to 0 for the mid-term scenarios in all sub-basins. Hence, the possible positions of the future variable distributions are outside the probable values corresponding to the historical distribution and nonstationarity should be considered. In relation to the scale and shape parameters, they do not shift homogeneously under climate change scenarios throughout the river basin and each sub-basin should be evaluated separately. Nevertheless, we suggest that the common assumption of a constant shape parameter could not be accurate in some of these sub-basins (Sueca, Alarcon-lower), which showed low values of the OVL for this parameter. To cope with the nonstationarity of climate, an interesting challenge is the definition of nonstationary standardized drought indices, in which some parameters of the distribution may vary in accordance with time or incorporate climate indices as covariates (Wang et al., 2015; Li et al., 2015).

Finally, our results show a huge uncertainty with regard to the future availability of water resources in the basin. This is consistent with the dispersion observed in the literature in assessments of future precipitation and temperature in Mediterranean areas. For example, Mourato et al. (2015) found changes in precipitation ranging from +1.5 to −65 % and an increase in temperature from +2.7 to +5.9°C for the Sado and Guadiana basins in Southern Portugal, whilst Senatore et al. (2011) found an increase in the average annual temperature between +3.5 C and +3.9 C and a decrease between 9% and 21% in the cumulative annual precipitation for the Crati basin in Southern Italy. In the Jucar basin, Chirivella Osma et al. (2015) found that the impact of climate scenarios on water resources showed a great degree of dispersion (ranging from -13.45% to 18.1% with a mean value of -2.13%) and, more recently, Marcos-Garcia and Pulido-Velazquez (2017) quantified this impact between -33.6% and 5.5% in the short-term and -43.5% and 2% in the mid-term.

7 Conclusions

Relative standardized indices have been used to assess climate change impacts on meteorological and hydrological droughts in the Jucar river basin, a Mediterranean basin in Eastern Spain with a gradient of climatic areas: from continental (upper basin) to Mediterranean (lower basin), with a transition in the mid basin.

To compare the dry spells between the historical and future conditions, we have used a combination of relative standardized indices. In order to enhance the capabilities of the standardized indices for the climatic and catchment conditions of the case study, we have improved PET estimation and the hydrological simulation of low-flow conditions. Finally, we have characterized the uncertainty and shifts of the assumed distribution of the parameters for the statistical representation of the indices under climate change scenarios.

The results have shown that the climate change scenarios lead to a general increase in the severity of both meteorological and hydrological droughts, due to the combined effects of rainfall reduction and evapotranspiration increase. Although the Standardized Precipitation Index (SPI) and the Standardized Precipitation Evapotranspiration Index (SPEI) show similar values for the historical period, under climate change scenarios the SPI could underestimate drought intensity and magnitude. Short-term scenarios presented droughts of lower magnitude and intensity than those identified for the mid-term scenarios. Our results also suggest that the areas where most of the water resources in the basin are located (inner areas) are more prone to suffer an increase in drought severity under climate change, which would get worse in the mid-term. This fact may play an important role in the design of future drought management plans and adaptation strategies. The deep uncertainty associated with the assessment of the potential effects of climate change on water resource systems (Wilby and Dessai, 2010) calls for a sound combination of conventional top–down analysis and bottom–up approaches for designing robust and dynamic adaptation plans at the local scale (e.g. Brown and Wilby 2012; Girard et al., 2015).

Acknowledgments

This study has been supported by the IMPADAPT project (CGL2013-48424-C2-1-R) with Spanish MINECO (Ministerio de Economía y Competitividad) and European FEDER funds. The authors thank AEMET (Spanish Meteorological Office) and University of Cantabria for the data provided for this work (dataset Spain02).

References

Agnew CT. 2000. Using the SPI to identify drought. Drought Network News 12(1): 6–1

Alley, W.M. 1984. The Palmer Drought Severity Index: Limitations and Assumptions. Journal of Climate and Applied Meteorology. 23: 1100-1109.

Anderson R.L. 1941. Serial correlation in the analysis of time series. Retrospective Theses and Dissertations. Paper 12880.

Barker L.J., Hannaford J., Svensson C. and Tanguy. 2015. A preliminary assessment of meteorological and hydrological drought indicators for application to catchments across the UK, in Andreu J. et al., DROUGHT. Research and Science-Policy Interfacing, 231-236. Ed. Balkelma. CRC Press, Netherlands

Bates, B.C., Z.W. Kundzewicz, S. Wu and J.P. Palutikof. 2008. Climate Change and water. Eds. IPCC Secretariat, Geneva, 210 pp.

Beguería, S., Vicente-Serrano, S. M., Reig, F. and Latorre, B. 2014. Standardized precipitation evapotranspiration index (SPEI) revisited: parameter fitting, evapotranspiration models, tools, datasets and drought monitoring. Int. J. Climatol., 34: 3001–3023. doi:10.1002/joc.3887

Brown, C. and Wilby, R. L. (2012), An alternate approach to assessing climate risks, Eos Trans. AGU, 93(41), 401.

Burke E. and Brown S.J. 2007. Evaluating uncertainties in the projection of future drought. Journal of Hydrometeorology. 2007. DOI: 10.1175/2007JHM929.1

Camargo A.P., Marin F.R., Sentelhas P.C., Picini A.G. 1999. Adjust of the Thornthwaite's method to estimate the potential evapotranspiration for arid and superhumid climates, based on daily temperature amplitude. Rev. Bras. Agrometeorol. 7 (2), 251-257 (in Portuguese with English summary)

Canty A., Ripley B. 2015. Bootstrap functions. https://cran.r-project.org/web/packages/boot/boot.pdf Accessed 29 June 2015

Chirivella Osma, V., Capilla Romá, J.E., Pérez Martín, M.A. 2015. Modelling regional impacts of climate change on water resources: the Júcar basin (Spain). Hydrological Sciences Journal, 60:1, 30-49, DOI: 10.1080/02626667.2013.866711

CHJ, 2007. Plan especial de alerta y eventual sequía en el ámbito de la Confederación Hidrográfica del Júcar. Confederación Hidrográfica del Júcar. Retrieved from www.chj.es. Last access: December 2015 (in Spanish)

CHJ, 2015. Plan Hidrológico de Cuenca. Demarcación Hidrográfica del Júcar. Confederación Hidrográfica del Júcar. Retrieved from www.chj.es. Last access: December 2015 (in Spanish)

Christensen O.B., Gutowski W.J., Nikulin G. and Legutke S. 2014. CORDEX Archive design. Available at http://cordex.dmi.dk/. Last access: December 2015

Coles S. 2001. An introduction to statistical modeling of extreme values. Springer, London.

Dai, A. 2011. Drought under global warming: a review. WIREs Clim Change, 2: 45–65. doi: 10.1002/wcc.81

Dai, A. 2013. Increasing drought under global warming in observations and models. Nature Clim. Change 3, 52-58.

Diffenbaugh N.S, Giorgi F. 2012. Climate change hotspots in the CMIP5 global climate model ensemble. Clim Change. 2012; 114(3-4): 813–822. doi: 10.1007/s10584-012-0570-x

Dracup, J.A., Lee, K.S., Paulson, E.G. 1980. On the definition of droughts. Water Resour. Res. 16 (2), 297-302.

Duan K., Mei Y. 2014. Comparison of meteorological, hydrological and agricultural drought responses to climate change and uncertainty assessment. Water Resour Manage (2014) 28:5039–5054 DOI 10.1007/s11269-014-0789-6

Dubrovsky M., Svoboda M.D., Trnka M., Hayes M.J., Wilhite D.A., Zalud Z., Hlavinka P. 2009. Application of relative drought indices in assessing climate-change impacts on drought conditions in Czechia. Theor Appl Climatol (2009) 96:155-171 DOI 10.1007/s00704-008-0020-x

Efron B. 1979. Bootstrap methods: another look at the jackknife. The Annals of Statistic. 1979, Vol. 7, No. 1, 1-26.

Estrela T., Sahuquillo, A. 1985. Modeling the response hydrograph of subsurface flow. Multivariate Analysis of the Hydrologic Processes, Proceedings of Fourth International Hydrology Simposium. July 15-17, 1987. Colorado State University, Fort Collins, USA.

Estrela T., Cabezas Calvo-Rubio F., Estrada Lorenzo F. La evaluación de los recursos hídricos en el Libro Blanco del Agua en España .Ingeniería del agua, [S.l.], v. 6, n. 2, jun. 1999. ISSN 1886-4996

Forzieri G., Feyen L., Rojas R., Flörke M., Wimmer F., Bianchi A. 2014. Ensemble projections of future streamflow droughts in Europe. Hydrol. Earth Syst. Sci., 18, 85–108, 2014

Fowler, H. J., Blenkinsop, S. and Tebaldi, C. (2007), Linking climate change modelling to impacts studies: recent advances in downscaling techniques for hydrological modelling. Int. J. Climatol., 27: 1547–1578. doi:10.1002/joc.1556

Fowler K. J. A., Peel M. C., Western A. W., Zhang L., Peterson T. J. (2016). Simulating runoff under changing climatic conditions: Revisiting an apparent deficiency of conceptual rainfall-runoff models, Water Resour. Res., 52, doi:10.1002/2015WR018068.

Girard, C., Pulido-Velazquez, M., Rinaudo, J-D., Pagé, C., Caballero, Y. 2015. Integrating top-down and bottom-up approaches to design global change adaptation at the river basin scale. *Global Environmental Change*, Volume 34, September 2015, Pages 132–146. doi:10.1016/j.gloenvcha.2015.07.002

Gudmundsson, L., Bremnes, J. B., Haugen, J. E., and Engen-Skaugen, T. 2012. Technical Note: Downscaling RCM precipitation to the station scale using statistical transformations – a comparison of methods. Hydrol. Earth Syst. Sci., 16, 3383-3390. doi:10.5194/hess-16-3383-2012

Hayes, M., D.A. Wilhite, M. Svoboda, and O. Vanyarkho. 1999. Monitoring the 1996 drought using the Standardized Precipitation Index. Bulletin of the American Meteorological Society 80, 429-438.

Herrera S., Gutiérrez J.M., Ancell R., Pons M.R., Frías M.D., Fernández J. 2010. Development and analysis of a 50-year high-resolution daily gridded precipitation dataset over Spain (Spain 02). International Journal of Climatology. doi: 10.1002/joc.2256/

Hosking J.R.M., Wallis J.R., Wood E.F. 1985. Estimation of the generalized extreme-value distribution by the method of probability weighted moments. Technometrics, 27(3), 251-261, 1985

IPCC 2014a. Climate Change 2014: Impacts, Adaptation, and Vulnerability. Part A: Global and Sectoral Aspects. Contribution of Working Group II to the Fifth Assessment Report of the Intergovernmental Panel on Climate Change" [Field, C.B., V.R. Barros, D.J. Dokken, K.J. Mach, M.D. Mastrandrea, T.E. Bilir, M. Chatterjee, K.L. Ebi, Y.O. Estrada, R.C. Genova, B. Girma, E.S. Kissel, A.N. Levy, S. MacCracken, P.R. Mastrandrea, and L.L. White (eds.)]. Cambridge University Press, Cambridge, United Kingdom and New York, NY, USA. 1132 pp

IPCC, 2014b: Climate Change 2014: Synthesis Report. Contribution of Working Groups I, II and III to the Fifth Assessment Report of the Intergovernmental Panel on Climate Change [Core Writing Team, R.K. Pachauri and L.A. Meyer (eds.)]. IPCC, Geneva, Switzerland, 151 pp.

Katz R.W. 2013. Statistical methods for nonstationary extremes. Chapter 2, Extremes in a changing climate: Detection, analysis and uncertainty, A. AghaKouchak, D. Easterling, and K. Hsu, eds, Vol.65, Springer, New York.

Kay A.L., Davies H.N. 2008. Calculating potential evaporation from climate model data: a source of uncertainty for hydrological climate change impacts. Journal of Hydrology (2008) 358, 221-239

Kim C.J., Park M.J., Lee J.H. 2014. Analysis of climate change impacts on the spatial and frequency patterns of drought using a potential drought hazard mapping approach. Int. J. Climatol. 34: 61–80 (2014)

Li, H., Sheffield, J., & Wood, E. F. 2010. Bias correction of monthly precipitation and temperature fields from Intergovernmental Panel on Climate Change AR4 models using equidistant quantile matching. Journal of Geophysical Research: Atmospheres (1984–2012), 115(D10)

Li, J. Z., Y. X. Wang, S. F. Li, and R. Hu. 2015. A Nonstationary Standardized Precipitation Index incorporating climate indices as covariates, J. Geophys. Res. Atmos., 120, 12,082–12,095, doi:10.1002/2015JD023920.

Liu L., Hong Y., Looper J., Riley R., Yong B., Zhang Z., Hocker J., Shafer M. 2013. Climatological Drought Analyses and Projection Using SPI and PDSI: Case Study of the Arkansas Red River Basin. J. Hydrol. Eng. 2013.18:809-816.

Loukas A., Vasiliades L., Tzabiras J. 2008. Climate change effects on drought severity. Adv. Geosci., 17, 23–29.

Marcos-Garcia P., Pulido-Velazquez M. Cambio climático y planificación hidrológica: ¿es adecuado asumir un porcentaje único de reducción de aportaciones para toda la demarcación? Ingeniería del agua, [S.l.], v. 21, n. 1, p. 35-52, ene. 2017. ISSN 1886-4996 (in Spanish with English summary).

McKee, T. B., N. J. Doesken, and J. Kleist. 1993. The relationship of drought frequency and duration of time scales. Eighth Conference on Applied Climatology, American Meteorological Society, Jan17-23, 1993, Anaheim CA, 179-186.

Mishra, A.K., V.P. Singh, 2010. A review of drought concept J. Hydrol., 391 (2010), 202–216.

Mourato, S., Moreira, M. & Corte-Real, J. 2015. Water Resour Manage 29: 2377. doi:10.1007/s11269-015-0947-5

Palmer, W.C. 1965. Meteorological Drought. U.S. Weather Bureau, Washington, D.C. Research Paper. Nº45, 58 pp.

Pedro-Monzonís, M., Solera, A., Ferrer, J., Estrela, T., and Paredes-Arquiola, J., 2015. A review of water scarcity and drought indexes in water resources planning and management. J. Hydrol 527 (2015) 482-493, http://dx.doi.org/10.1016/j.jhydrol.2015.05.003

Pereira A.R., Pruitt W.O. 2004 .Adaptation of the Thornthwaite scheme for estimating daily reference evapotranspiration. Agricultural Water Management 66, 251-257.

Pérez-Martín, M.A., Batán, A., del-Amo, P., Moll, S. 2015. Climate change impact on water resources and droughts of AR5 scenarios in the Jucar River, Spain, in Andreu J. et al., DROUGHT. Research and Science-Policy Interfacing, 231-236. Ed. Balkelma. CRC Press, Netherlands

Pulido-Velázquez, M., Sahuquillo, A., Ochoa, JC., and Pulido-Velázquez, D., 2005. Modeling of stream-aquifer interaction: the embedded multireservoir model. J. Hydrology, 313(3-4), 166-181, 10.1016/j.jhydrol.2005.02.026

Pulido-Velazquez, M., S. Peña-Haro, A. Garcia-Prats, A. F. Mocholi-Almudever, L. Henriquez-Dole, H. Macian-Sorribes, A. Lopez-Nicolas, 2015. Integrated assessment of the impact of climate and land use changes on groundwater quantity and quality in Mancha Oriental (Spain). Hydrol. Earth Syst. Sci., 19, 1677–1693. doi:10.5194/hess-19-1677-2015

R Core Team. 2015. R: A language and environment for statistical computing. R Foundation for Statistical Computing, Vienna, Austria. URL https://www.R-project.org/

Salas, J.D., Delleur, J.W., Yevjevich, V. and Lane, W.L. 1980. Applied modeling of hydrologic time series. Water Resources Publications. Littleton, Colorado.

Salas J.D., Obeysekera J. 2014. Revisiting the concepts of return period and risk for nonstationary hydrologic extreme events. J.Hydrol.Eng. 2014.19:554-568

Sanz, D., Castaño, S., Cassiraga, E., Sahuquillo, A., Gómez-Alday, J. J., Peña, S., and Calera, A. 2011. Modeling aquifer-river interactions under the influence of groundwater abstraction in the Mancha Oriental System (SE Spain), Hydrogeol. J., 19, 475–487.

Sellers W. (1963) Potential evapotranspiration in arid regions. Journal of Applied Meteorology. Volume 3, 98-104

Senatore, A., Mendicino, G., Smiatek, G., Kuntsmann, H. 2011. Regional climate change projections and hydrological impact analysis for a Mediterranean basin in Southern Italy. Journal of Hydrology, Volume 399, Issues 1–2, Pages 70–92

Shukla, S., and A. W. Wood. 2008. Use of a standardized runoff index for characterizing hydrologic drought. Geophys. Res. Lett., 35, L02405, doi:10.1029/2007GL032487.

Stagge J. H., Tallaksen L.M., Gudmundsson L., Van Loon A. F., Stahl K. 2015. Candidate distributions for climatological drought indices (SPI and SPEI). International Journal of Climatology, Volume 35, Issue 13, 4027–4040.

Tallaksen, L.M. 1995. A review of baseflow recession analysis. J. Hydrol., 165, 349–370.

Tallaksen, L.M, & van Lanen, H.A.J. 2004. Hydrological Drought: Processes and estimation methods for streamflow and groundwater. Development in water science, no. 48. Elsevier.

Témez Peláez, J.R. 1977. Modelo matemático de transformación precipitación-aportación. ASINEL, 1977. (in Spanish)

Teutschbein, C. and Seibert, J., 2012. Bias correction of regional climate model simulations for hydrological climate-change impact studies: Review and evaluation of different methods. J. Hydrol., 16, 12–29, doi:10.1016/j.jhydrol.2012.05.052.

Thornthwaite, C. W. 1948. An approach toward a rational classification of climate. Geogr. Rev., 38, 55–94.

Törnros T., Menzel L. 2014. Addressing drought conditions under current and future climates in the Jordan River region. Hydrol. Earth Syst. Sci., 18, 305–318

Trajkovic S. (2005) Temperature-Based Approaches for Estimating Reference Evapotranspiration. Journal of Irrigation and Drainage Engineering. 10.1061/(ASCE)0733-9437(2005)131:4(316), 316-323

Vicente-Serrano S., González-Hidalgo J.C., De Luis M., Raventós J. 2004. Drought patterns in the Mediterranean area: the Valencia region (eastern Spain). Climate Research 26, 5-15

Vicente-Serrano S.M., Beguería S. and López-Moreno J.I. 2010. A multiscalar drought index sensitive to global warming: The Standarized Precipitation Evapotranspiration Index. Journal of Climate 23: 1696-1718

Wang D., Hejazi M., Cai X., Valocchi A. J. 2011. Climate change impact on meteorological, agricultural, and hydrological drought in central Illinois. Water Resources Research 47, W09527, doi:10.1029/2010WR009845

Wang, Y., Li, J., Feng, P., Hu, R. 2015. A Time-Dependent Drought Index for Non-Stationary Precipitation Series Water Resour Manage 29: 5631. doi:10.1007/s11269-015-1138-0

Weitzman, M. 1970. Measures of overlap of income distributions of white and negro families in the U.S. Technical Paper 22, Bureau of the Census.

Wilby, R. L., Dessai, S. 2010. Robust adaptation to climate change. Weather, 65: 180–185. doi: 10.1002/wea.543

Wilhite, D.A. 2000. Drought: A global assessment. Ed. Routledge.

Yevjevich V. 1967. An objective approach to definitions and investigations of continental hydrologic droughts. Hydrology papers. Nº 23. Colorado State University. Fort Collins, Colorado.

Zargar, A., Sadiq, R., Naser, B., and Khan, F. I. 2011. A review of drought indices. Environ. Rev., 19, 333–349

Zargar A., Sadiq R., Khan F. I. 2014. Uncertainty-driven characterization of climate change effects on drought frequency using enhanced SPI Water Resources Management 28, 15-40 DOI 10.1007/s11269-013-0467-0